Excitation-Dependent Long-Life Luminescent Polymeric Systems under Ambient Conditions

Yan Su,[+] Yongfeng Zhang,[+] Zhonghao Wang, Weichen Gao, Peng Jia, Dan Zhang, Chaolong Yang,* Youbing Li, Yanli Zhao*

Abstract: Organic room temperature luminescent materials present unique phosphorescence emission with long lifetime. However, a lot of these materials only emit single blue or green color in spite of external stimulation, whereas their color tunability is strictly limited. Herein, we report a rational design to extend the emission color range from blue to red by controlling the doping of simple pyrene derivatives into robust polymer matrix. The integration of these pyrene molecules in the polymer films enhances the intersystem crossing pathway, decreases the first triplet level of the system, and ensures the films with sensitive response to excitation energy, finally yielding excitation-dependent long-life luminescent polymeric systems under ambient conditions. By virtue of exceptional behavior, these materials were utilized as a versatile platform for constructing anti-counterfeiting patterns with multicolor interconversion, presenting a promising application potential in the field of information security.

Ultralong organic luminescence (UOL) materials have drawn great interests, as they show promising application potentials in biological imaging, photodynamic therapy, information storage, sensing, electroluminescent devices, and security protection.[1] A large variety of UOL materials with long lifetime and remarkable luminescent efficiency under ambient conditions have been developed by taking advantage of the mechanisms such as polymer aggregation, crystallization, halogen bonding, self-assembly, host-guest complexation, and H-aggregation.[2] Despite recent progress, developing advanced UOL materials still remains challenges in several aspects. First, the quantum yield of UOL materials is still low, because of inefficient spin-orbit coupling and undesignable triplet radiative transition rate.[3] Second, a lot of UOL materials are crystalline in nature, since the ordered aggregation states stabilize the triplet excitation energy and benefit their phosphorescence performance.[4] Such rigid and fragile crystalline forms are often difficult to be proceeded, hampering their further applications. Third, most of UOL materials emit blue or green light, whereas their color designability is strictly limited.[5] Thus, these issues need to be overcome in order to promote the applications of UOL materials to a higher stage.

It is well known that color-tunable luminescent materials can be widely used in many fields, including sensors, bio-markers, bioassay, anti-counterfeiting, and flexible electronics, on account of their unique photophysical properties.[6] Some representative UOL crystals with both long lifetime and high phosphorescent quantum yield have been explored,[7] and several fluorescent materials showing changeable emission colors have been reported.[8] However, developing excitation-dependent long-life luminescent polymer systems under ambient conditions has not been well studied to the best of our knowledge. In particular, achieving polymer-based luminescent systems with tunable afterglow colors from blue to red under ambient conditions is still highly challenging.

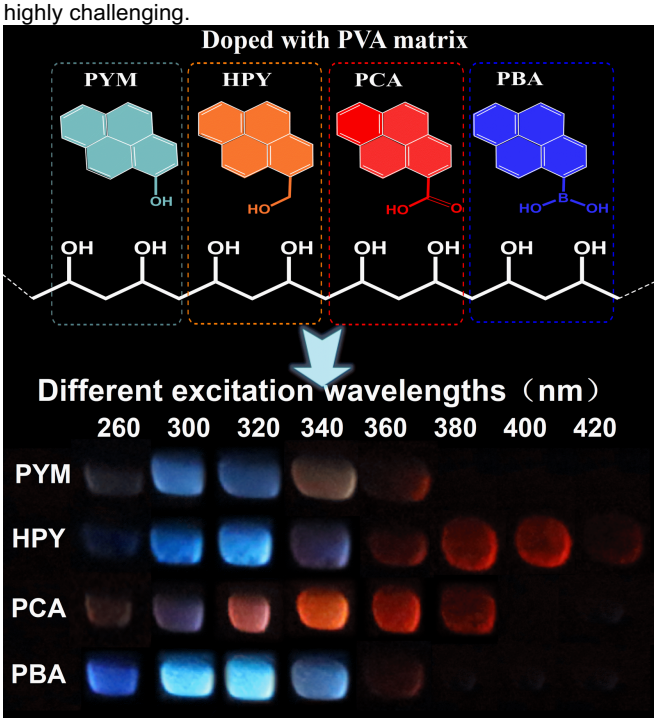

Figure 1. Molecular structures of PYM, HPY, PCA, PBA, and PVA, as well as corresponding UOL images of the doped PVA films under various excitation wavelengths.

Recently, we developed the irradiation-dependent UOL materials by doping a non-emission guest into polyvinyl alcohol (PVA) matrix, demonstrating effective turn-on UOL performance from triplet stabilization.[9] Different to this work, we herein report the excitation-dependent long-life luminescent polymer (ED-LFLP) systems that can simultaneously solve the issues of processability and color tunability under ambient conditions. By controlling the aggregative state and formation of hydrogen bonding interaction, we could preciously adjust the emission from different triplet states, and extend the afterglow colors of UOL materials into red range. These polymer-based UOL materials possess the advantage of easy solution processing on large, flexible, and transparent substrates, and thus are more useful for advanced applications. We applied these UOL polymers as a versatile platform in the interconversion of blue and red emission for dual-light responsive anti-counterfeiting.

[a] Y. Su, Y. Zhang, Z. Wang, W. Gao, P. Jia, D. Zhang, Y. Li, and Prof. Dr. C. Yang
School of Materials Science and Engineering, Chongqing University of Technology, Chongqing, 400054, P.R. China
E-mail: yclzjun@163.com
[b] Prof. Dr. C. Yang, and Prof. Y. L. Zhao
Division of Chemistry and Biological Chemistry, School of Physical and Mathematical Sciences, Nanyang Technological University, 21 Nanyang Link, Singapore 637371
E-mail: zhaoyanli@ntu.edu.sg
[+] These authors contributed equally to this work.

Supporting information for this article is given via a link at the end of the document.

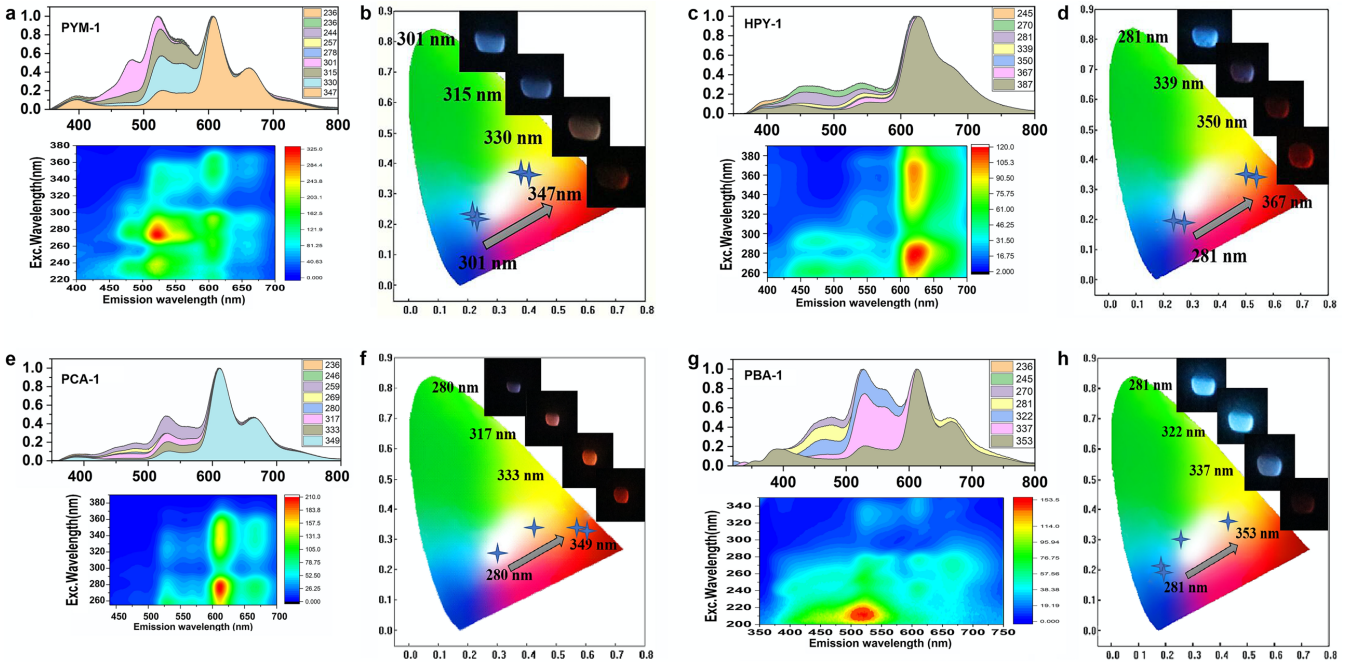

Figure 2. (a) Excitation–phosphorescence mapping of PYM-1 doped into PVA at 300 K. The upper figure shows the phosphorescence spectra of the film under different excitation wavelengths. (b) Trajectory of color modulation, recorded by the change of the excitation from 301 to 347 nm, in the CIE coordinate diagram. The inset images show the UOL photographs of the film taken under the excitation at 301, 315, 330 and 347 nm, respectively. (c) Excitation–phosphorescence mapping of HPY-1 doped into PVA at 300 K. (d) Trajectory of color modulation, recorded by the change of the excitation from 281 to 367 nm, in the CIE coordinate diagram. The inset images show the UOL photographs of the film taken under the excitation at 281, 339, 350 and 367 nm, respectively. (e) Excitation–phosphorescence mapping of PCA-1 doped into PVA at 300 K. (f) Trajectory of color modulation, recorded by the change of the excitation from 280 to 349 nm, in the CIE coordinate diagram. The inset images show the UOL photographs of the film taken under the excitation at 280, 317, 333 and 349 nm, respectively. (g) Excitation–phosphorescence mapping of PBA-1 doped into PVA at 300 K. (h) Trajectory of color modulation, recorded by the change of the excitation from 281 to 353 nm, in the CIE coordinate diagram. The inset images show the UOL photographs of the film taken under the excitation at 281, 322, 337 and 353 nm, respectively.

The ED-LFLP systems were prepared by doping various pyrene derivatives (Figure 1), namely 1-pyrenemethanol (PYM), 1-hydroxypyrene (HPY), 1-pyrenecarboxylic acid (PCA), and 1-pyrenylboronic acid (PBA), into the PVA matrix, giving effectively suppressed non-radiative deactivation within the rigid amorphous environment.[9] After drop-casting the aqueous solution of these hybrid materials onto substrates and heating them at 65 °C for 4 h, the dopants form robust hydrogen bonds with the PVA matrix, as evidenced by FT-IR (Figure S1) and TGA (Figure S2). These films showed simultaneous dual emission of fluorescence and phosphorescence in ambient conditions (Figure S3).

Interestingly, upon UV light irradiation with different wavelengths, the films emitted bright phosphorescence with different colors. Taking PYM-PVA film as an example, it showed blue phosphorescence upon excited by 260 nm UV light. When increasing the wavelengths of excitation source from 300 to 420 nm, the emission color changed from blue to yellow, and then to deep red (Figure 1). Other hybrid materials also exhibited similar behavior with the emission color change from blue to red upon increasing the excitation wavelengths. These results revealed distinctive phenomena from other conventional UOL materials in terms of large color-tunable range.

To understand the emission behavior, UV-vis spectra of the doped polymer films were measured (Figure S4), which showed multiple strong peaks assignable to the absorption from ground states to various singlet excited states. Accordingly, we also measured the excitation–phosphorescence spectra with different excitation wavelengths. Upon the excitation at 236 nm, the emission spectra of the PYM-PVA film exhibited six peaks at 397, 482, 523, 559, 606, and 663 nm (Figure 2a,b), with Commission International de l'Eclairage (CIE) coordinate of (0.187, 0.210). As increasing the excitation wavelength from 236 to 347 nm, the relative intensity decreased in blue and green range, while the intensity of red range remained almost unchanged. As a consequence, the CIE coordinate of the film shifted to (0.394, 0.382). In the HPY-PVA film, blue and green emissions were rather balanced, and they simultaneously decreased upon increasing the excitation wavelengths (Figure 2c,d), yielding a large CIE variation from (0.191, 0.178) to (0.525, 0.336). Upon excited by 280 nm, the initial blue emission in the PCA-PVA film was very weak, making the CIE coordinate close to the white-light range (Figure 2e,f). As increasing the excitation wavelength, the blue and green emissions rapidly decreased, endowing the film with orange and red emission with the CIE coordinate varying from (0.300, 0.268) to (0.594, 0.371). In contrast, the initial blue and green emissions in the PBA-PVA film were strong, and their changes were less obvious than the other three films upon increasing the excitation wavelength (Figure 2g,h). The PYM-PVA, HPY-PVA, PCA-PVA, and PBA-PVA films showed relatively long lifetimes of 0.63, 0.46, 0.29, and 0.67 s under the excitation at 320 nm, while the lifetimes changed obviously to 0.21, 0.10, 0.13, and 0.32 s under the excitation at 340 nm, respectively (Figure S5 and Table S1). Such small alteration (from 320 to 340 nm) of the excitation wavelength results in a significant difference in the spectra and a

dramatic decrease in the lifetime, indicative of sensitive response of the doped polymer films to the excitation energy. Meanwhile, the PYM-1, HPY-1, PCA-1, and PBA-1 films showed relatively high phosphorescent quantum yields of 5.1%, 11.9%, 19.7%, and 15.0% under 300 nm excitation, respectively. Photophysical data of these films are shown in Table S1.

The mechanism for the excitation-dependent luminescent behavior of the doped polymers was further investigated in detail. In this study, there are two proposed mechanisms that can cause the afterglow color change from blue to red upon increasing the excitation wavelength. The first one is based on the Anti-Kasha's Rule,[10] and the second is related to the isolated-aggregation state.[11] In order to deeply understand the mechanism of excitation-dependent luminescent behavior of the doped polymers, we intentionally controlled the doping contents of the pyrene derivatives and measured corresponding emission spectra. Taking PCA-PVA as an example, we doped PCA with the concentration of 0.1, 0.3, 0.5, 1, and 3 mg mL^{-1} into 30 mg mL^{-1} PVA solution and defined the resulting films as PCA-0.1, PCA-0.3, PCA-0.5, PCA-1, and PCA-3, respectively. The fluorescence of the PCA-doped films exhibited three peaks at 383, 403, and 425 nm (Figure S6), which remained almost the same as increasing the doping content of PCA. The phosphorescence of the PCA-doped films showed four peaks at 474, 529, 612, and 667 nm. As increasing the doping content of PCA, the intensity of peaks at 529, 612, and 667 nm significantly increased, whereas the peak at 474 nm gradually vanished, suggesting that more and more excitation energies flow into low-energy emission pathway.[12,13] We also measured the phosphorescence spectra of PYM-PVA under variable excitation wavelengths (Figure S7). Under low doping contents of 0.1 and 0.3 mg mL^{-1}, the peak at 478 nm held a large proportion in the phosphorescence spectra upon excited with high energies, whereas the peak intensity at 478 and 522 nm significantly decreased as increasing the excitation wavelength, yielding an obvious blue-to-red transition of the films. Thus, the blue luminescence could be ascribed to the phosphorescence of isolated molecules. When the doping contents were in a range of 0.5 to 5 mg mL^{-1}, the peaks at 522 and 607 nm had the largest proportion in the phosphorescence spectra under excitation with high energy, but the intensity of the former peak gradually decreased upon increasing the excitation wavelength. These results indicate that, since the performance of polymer films is strongly concentration-dependent, the isolated-aggregation state should be reasonable mechanism to trigger the unique luminescence in these systems. If the luminescence phenomenon is caused by the Anti-Kasha's Rule, the polymeric systems cannot exhibit concentration dependency, simply because the emission from higher excited states would not be affected by the concentration.[10] Meanwhile, the phosphorescence properties of these four pyrene molecules at 77 K only exhibited immutable blue color even when the excitation wavelength was largely changed (Figure S8). The efficiency of the red emission process is suppressed at low temperature, further confirming that the excitation-dependent luminescence performance is induced by the isolated-aggregation state. Obvious change of the afterglow color over time and remarkable difference of time-resolved emission spectra under 300nm and 360nm excitation further reveal the simultaneous presence of isolated and aggregated states in these doped film systems (Figures S9 and S10).

To gain deeper insight into the unique optical properties, a set of control experiments was carried out. We measured the phosphorescence spectra of PYM-PVA system with low doping contents under variable excitation wavelengths. Under low doping contents of 0.001 and 0.01 mg mL^{-1}, the peak at 463 nm held a large proportion in the phosphorescence spectra upon excitation with high energy, whereas the peak intensity at 463 and 525 nm significantly decreased upon increasing the excitation wavelength, yielding an obvious blue-to-red transition of the films (Figure S11). The PYM-0.001 film showed long lifetime of 0.72 s under the excitation at 320 nm. Thus, the blue afterglow could be ascribed to the phosphorescence of isolated molecules. Meanwhile, the phosphorescence of PYM-PVA films with high doping contents under ambient conditions was also measured (Figure S12). When the doping contents were 30 mg mL^{-1} or higher, the peak intensity at 478 and 522 nm was obviously suppressed and the peak at 607 nm was dominant. The phosphorescence under high doping contents only exhibited immutable red emission even when the excitation wavelength was significantly changed. Therefore, the red afterglow should be ascribed to the phosphorescence of aggregated state.

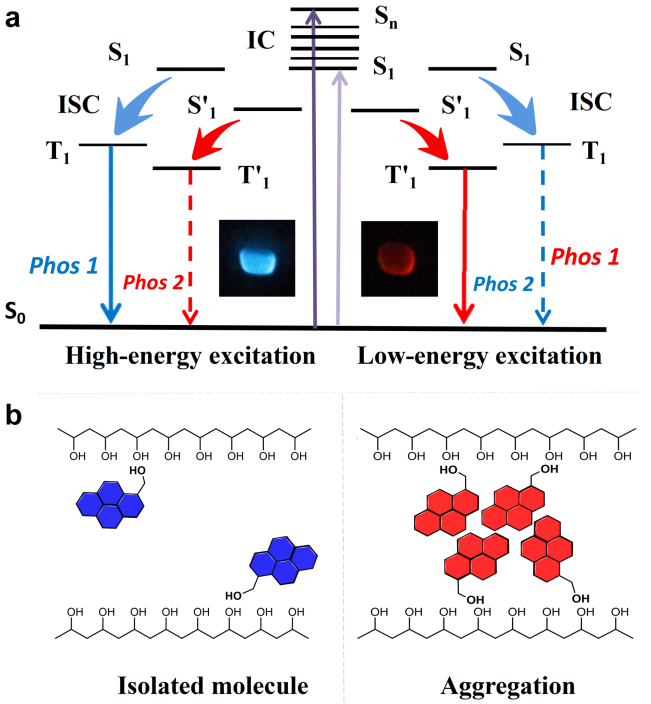

Figure 3. (a) Schematic diagram for the energy levels of doped polymer films, suggesting different emission pathways by high- and low-energy excitations. (b) Schematic diagrams of the isolated molecular state and aggregation state of PYM doped PVA polymer.

In the doped polymer films, there are two emission centers at the same time (Figure 3). The first one belongs to the isolated molecular state, and the second is from the aggregation state. The first singlet excited state (S_1, S_1') and the first triplet level (T_1, T_1') of the aggregation state are lower than those of the isolated state (Figure 3a), as confirmed by the time-dependent density functional theory (TD-DFT) calculations (discussed later). Under low doping contents, the film is dominated by isolated molecular state, and the photonic channel is primarily from S_1 to T_1. At this moment, the aggregation state is very little. Thus, the blue afterglow is dominant after the removal of the high-energy excitation source (such as 254 nm). When increasing the doping contents, the isolated molecular state gradually decreases, and the aggregation state gradually increases. At higher doping contents, the isolated molecular state becomes less populated. At this moment, the emission center is dominated by the

aggregation state, and the photonic channel is primarily from S'_1 to T'_1. Thus, the red afterglow emission is observed after the removal of the low-energy excitation energy source (such as 365 nm).

To further understand the relationship between the aggregation and emission behavior, we performed TD-DFT calculations of singlet and triplet energy levels of the doped films (Figure S13).[14] In the monomer state, the intersystem crossing (ISC) from singlet to triplet states is strict with limited ISC pathways. Upon the aggregation, the energy difference between S_n (n > 1) and S_1 significantly decreases, the energy difference between T_n (n > 1) and T_1 significantly decreases, and the energy levels of the emission excited states tend to converge with the increment of the aggregation number (e.g., from dimer to trimer), clearly demonstrating an aggregative emission. This trend provides more and efficient ISC pathways at upper triplet levels, and thus could regulate the emission from different triplet states by altering the excited energy. This is the essence of the excitation-dependent UOL behavior of the doped polymer films. Meanwhile, the excitation-dependent luminescent phenomenon was not observable through doping the pyrene derivatives into PVA-89 (89% hydrolyzed PVA), PVAc (polyvinyl acetate), and PMMA (polymethyl methacrylate), respectively (Figure S14). Therefore, the strong intermolecular interaction (e.g., hydrogen bonding) and the formation of the aggregation state play central roles in realizing excitation-dependent luminescence of these polymeric systems under ambient conditions. In addition, different aggregation states of polymer films with low and high doping contents were also supported by atomic force microscope studies (Figure S15).

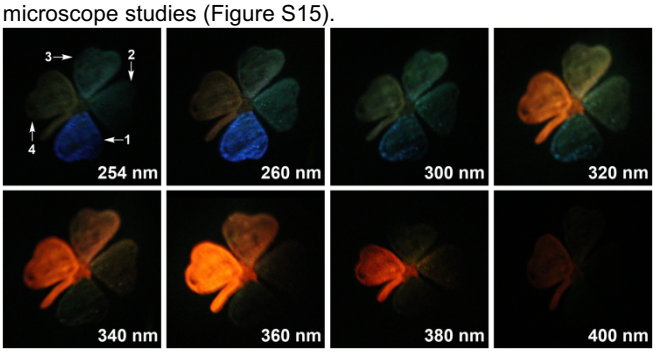

Figure 4. Multicolor clover pattern on a paper drawn by doped-polymer inks upon the irradiation followed by the removal of UV light. Numbers 1-4 refer to PBA-PVA, HPY-PVA, PYM-PVA, and PCA-PVA, respectively.

The development of stimulus-responsive luminescent materials has attracted tremendous interests on account of their promising applications in the security protection such as information storage, encryption, and anti-counterfeiting. It is really meaningful to develop multiple stimulus-responsive luminescent materials with widely adjustable and highly distinctive emission colors for high-level information storage and security protection. The present doped polymer films with high transparency in visible range (Figure S16) and largely tunable emission from blue to red could be used as security inks to meet above requirements. Importantly, when the film thickness reaches a certain value (several hundreds of nanometers on PET or micrometers on glass), the films could be easily peeled off from the substrates to yield free-standing films. The size and shape of the free-standing films would completely depend on those substrates. Thus, our method could offer high-quality films either on substrates or in free-standing forms, with synthetically controlled thickness, size and shape. The prepared free-standing films were highly robust with a tensile strength of 4.89 MPa (Figure S17). For instance, the PYM-PVA film showed suppressed blue and green emission, and strongly enhanced red emission under varied irradiation wavelength, probably due to film orientation-induced re-arrangement of doped molecules (Figure S18).

To demonstrate the anti-counterfeiting application of the ED-LFLP system, we prepared multicomponent patterns by using our doped polymers. The procedure is described as follows (Figure S19). Upon the irradiation followed by the removal of 260 nm UV light, the petals drawn by PCA-PVA, PYM-PVA/HPY-PVA, and PBA-PVA inks emitted red, sky-blue, and blue luminescence, respectively (Figure 4). In sharp contrast, upon the irradiation and the removal of 360 nm UV light, these parts emitted strong or weak red luminescence. As compared with conventional multicolor patterning luminescent materials, the present system possesses the advantage of high discriminability and easy preparation. These unique features make the doped polymer films highly promising for future anti-counterfeiting and security applications.

In summary, we have developed a rational strategy to achieve excitation-dependent phosphorescence emission under ambient conditions using metal-free and heavy atom-free amorphous organic materials through the formation of controlled aggregation to increase the ISC pathways. Doping content-dependent spectral measurements and theoretical calculations indicate different triplet states with various ISC pathways upon the aggregation, ensuring the doped polymer films with sensitive response to the excitation energy. By virtue of the unique UOL features, a multicolor demonstration has been established by utilizing the doped polymers as a versatile platform toward future anti-counterfeiting applications. We anticipate that this doping strategy for preparing ED-LFLP systems could find wide applications in biosensing, light-emitting devices, data storage, and information security.

Acknowledgements

This work was financially supported by the National Natural Science Foundation of China (21875025), the special program of Chongqing Science and Technology Commission (cstc2018jcyjAX0296 and cstc2017zdcyzdyfX0007), Innovation Research Group at Institutions of Higher Education in Chongqing (CXQT19027), and the Science and Technology Research Program of Chongqing Municipal Education Commission (KJZD-K201801101 and KJ1709222). The research was also supported by the Singapore Agency for Science, Technology and Research (A*STAR) AME IRG grant (A1883c0005).

Keywords: aggregation • anti-counterfeiting • doped polymer films • excitation dependence • long-life luminescence

[1] a) H. Al-Attar, A. Monkman, *Adv. Funct. Mater.* **2012**, *22*, 3824; b) S. Hirata, K. Totani, J. Zhang, T. Yamashita, H. Kaji, S. Marder, T. Watanabe, C. Adachi, *Adv. Funct. Mater.* **2013**, *23*, 3386; c) Z. An, C. Zheng, Y. Tao, R. Chen, H. Shi, T. Chen, Z. Wang, H. Li, R. Deng, X. Liu, W. Huang, *Nat. Mater.* **2015**, *14*, 685; d) S. Hirata, *Adv. Opt. Mater.* **2017**, *5*, 1700116; e) N. Gan, H. Shi, Z. An, W. Huang, *Adv. Funct. Mater.* **2018**, *28*, 1802657; f) R. Gao, X. Mei, D. P. Yan, R. Liang, M. Wei, *Nat. Commun.* **2018**, *9*, 2798.

[2] a) O. Bolton, K. Lee, H.-J. Kim, K. Y. Lin, J. Kim, *Nat. Chem.* **2011**, *3*, 205; b) D. Lee, O. Bolton, B. C. Kim, J. H. Youk, S. Takayama, J. Kim, *J. Am. Chem. Soc.* **2013**, *135*, 6325-6329; c) H. Chen, X. Ma, S. Wu, H. Tian, *Angew.*

Chem. Int. Ed. **2014**, *53*, 14149–14152; d) W. Zhao, Z. He, J. W. Y. Lam, Q. Peng, H. Ma, Z. Shuai, G. Bai, J. Hao, B. Z. Tang, *Chem* **2016**, *1*, 592; e) R. Kabe, C. Adachi, *Nature* **2017**, *550*, 384; f) D. Li, F. Lu, J. Wang, W. Hu, X.-M. Cao, X. Ma, H. Tian, *J. Am. Chem. Soc.* **2018**, *140*, 1916; g) R. Gao, X. Fang, D. Yan, *J. Mater. Chem. C* **2018**, *6*, 4444; h) B. Zhou, D. Yan, *Adv. Funct. Mater.* **2019**, *29*, 1807599.

[3] Z. He, W. Zhao, J. W.Y. Lam, Q. Peng, H. Ma, G. Liang, Z. Shuai, B. Z. Tang, *Nat. Commun.* **2017**, *8*, 416.

[4] H. Chen, X. Yao, X. Ma, H. Tian, *Adv. Optical Mater.* **2016**, *4*, 1397.

[5] a) R. Gao, D. Yan, *Chem. Sci.* **2017**, *8*, 590; b) S. Tian, H. Ma, X. Wang, A. Lv, H. Shi, Y. Geng, J. Li, F. Liang, Z.-M. Su, Z. An, W. Huang, *Angew. Chem. Int. Ed.* **2019**, *58*, 6645; c) M. Louis, H. Thomas, M. Gmelch, A. Haft, F. Fries, S. Reineke, *Adv. Mater.* **2019**, *31*, 1807887.

[6] a) H. Lee, J. Kim, H. Kim, J. Kim, S. Kwon, *Nat. Mater.* **2010**, *9*, 745; b) J. Lee, P. W. Bisso, R. L. Srinivas, J. J. Kim, A. J. Swiston, P. S. Doyle, *Nat. Mater.* **2014**, *13*, 524; c) Z. T Zhang, K. P. Guo, Y. M. Li, X. Y. Li, G. Z. Guan, H. P. Li, Y. F. Luo, F. Y. Zhao, Q. Zhang, B. Wei, Q. B. Pei, H. S. Peng, *Nat. Photon.* **2015**, *9*, 233.

[7] a) L. Bian, H. Shi, X. Wang, K. Ling, H. Ma, M. Li, Z. Cheng, C. Ma, S. Cai, Q. Wu, N. Gan, X. Xu, Z. An, W. Huang, *J. Am. Chem. Soc.* **2018**, *140*, 10734; b) B. Zhou, D. Yan, *Angew. Chem. Int. Ed.* **2019**, *58*, 15128-15135s; c) W. Zhao, T. S. Cheung, N. Jiang, W. Huang, J. W. Y. Lam, X. Zhang, Z. He, B. Z. Tang, *Nat. Commun.* **2019**, *10*, 1595; d) H. Shi, L. Song, H. Ma, C. Sun, K. Huang, A. Lv, W. Ye, H. Wang, S. Cai, Y. Zhang, Z. An, W. Huang, R. Zheng, *J. Phys. Chem. Lett.* **2019**, *10*, 595.

[8] a) Z. Mao, Z. Yang, Y. Mu, Y. Zhang, Y. F. Wang, Z. G. Chi, C. Lo, S. w. Liu, A. Lien, J. R. Xu, *Angew. Chem. Int. Ed.* **2015**, *54*, 6270; b) Y. Yang, K. Z. Wang, D. Yan, *ACS Appl. Mater. Interfaces* **2017**, *9*, 17399; c) Y. Su, J. H. Yu, Y. B. Li, S. F. Z. Phua, G. F. Liu, W. Q. Lim, X. Z. Yang, R. Ganguly, C. Dang, C. L. Yang, Y. L. Zhao. *Commun. Chem.* **2018**, *1*, 12; d) C. Sun, X. Wang, Z. Cheng, Q. Wu, S. Cai, L. Gu, N. Gan, H. Shi, Z. An, H. Shi, W. Huang, *J. Phys. Chem. Lett.* **2018**, *9*, 335; e) Z. Cheng, H. Shi, H. Ma, L. Bian, Q. Wu, L. Gu, S. Cai, X. Wang, W. W. Xiong, Z. An, W. Huang, *Angew. Chem. Int. Ed.* **2018**, *57*, 678.

[9] Y. Su, S. Z. F. Phua, Y. Li, X. Zhou, D. Jana, G. Liu, W. Q. Lim, W. K. Ong, C. Yang, Y. Zhao, *Sci. Adv.* **2018**, *4*, eaas9732.

[10] a) H. Qian, M. E. Cousins, E. H. Horak, A. Wakefield, M. D. Liptak, I. Aprahamian, *Nat. Chem.* **2017**, *9*, 83; b) L. Paul, T. Moitra, K. Ruud, S. Chakrabarti, *J. Phys. Chem. Lett.* **2019**, *10*, 369; c) X. Qiao, Y. Liu, J. Yao, X. He, P. Lu, D. Ma, *J. Phys. Chem. C* **2019**, *123*, 5761; d) Y. Gong, Y. Zhou, B. Yue, B. Wu, R. Sun, S. Qu, L. Zhu, *J. Phys. Chem. C* **2019**, *123*, 22511.

[11] a) J. Guo, X.-L. Li, H. Nie, W. Luo, S. Gan, S. Hu, R. Hu, A. Qin, Z. Zhao, S.-J. Su, B. Z. Tang, *Adv. Funct. Mater.* **2017**, *27*, 1606458; b) J. Guo, X.-L. Li, H. Nie, W. Luo, R. Hu, A. Qin, Z. Zhao, S.-J. Su, B. Z. Tang, *Chem. Mater.* **2017**, *29*, 3623; c) L. Gu, H. Shi, L. Bian, M. Gu, K. Ling, X. Wang, H. Ma, S. Cai, W. Ning, L. Fu, H. Wang, S. Wang, Y. Gao, W. Yao, F. Huo, Y. Tao, Z. An, X. Liu, W. Huang, *Nat. Photon.* **2019**, *13*, 406; d) J. Guo, J. Fan, L. Lin, J. Zeng, H. Liu, C.-K. Wang, Z. Zhao, B. Z. Tang, *Adv. Sci.* **2019**, *6*, 1801629.

[12] N. Jiang, G.-F. Li, B.-H. Zhang, D.-X. Zhu, Z.-M. Su, M. R. Bryce, *Macromolecules* **2018**, *51*, 4178.

[13] Y. Zhang, H. Yang, H. Ma, G. Bian, Q. Zang, J. Sun, C. Zhang, Z. An, W.-Y. Wong, *Angew. Chem. Int. Ed.* **2019**, *58*, 8773.

[14] a) Y. Tao, R. Chen, H. Li, J. Yuan, Y. Wan, H. Jiang, C. Chen, Y. Si, C. Zheng, B. Yang, G. Xing, W. Huang, *Adv. Mater.* **2018**, *30*, 1803856; b) Y. Xiong, Z. Zhao, W. Zhao, H. Ma, Q. Peng, Z. He, X. Zhang, Y. Chen, X. He, J. W. Y. Lam, B. Z. Tang, *Angew. Chem. Int. Ed.* **2018**, *57*, 7997.

COMMUNICATION

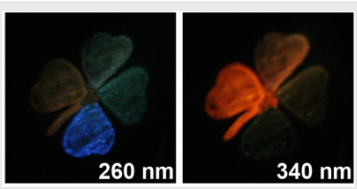

A rational design to achieve the excitation-dependent long-life luminescent polymer systems at ambient conditions by tuning the aggregation state of phosphors in polyvinyl alcohol films is developed, showing a promising application for multicolor patterning with high distinguishability and easy processing property.

Yan Su, Yongfeng Zhang, Zhonghao Wang, Weichen Gao, Peng Jia, Dan Zhang, Chaolong Yang, Youbing Li, Yanli Zhao**

Page No. – Page No.

Excitation-Dependent Long-Life Luminescent Polymeric Systems under Ambient Conditions